Available online at www.sciencedirect.com
ScienceDirect
Journal of the European Ceramic Society 26 (2006) 3357–3363
www.elsevier.com/locate/jeurceramsoc

Cyclic fatigue and lifetime of a concrete refractory

F. Thummen, C. Olagnon *, N. Godin

INSA-GEMPPM, CNRS-UMR5510, 20av Albert Einstein, 69621 Villeurbanne Cedex, France

Received 30 June 2005; received in revised form 27 October 2005; accepted 6 November 2005
Available online 24 March 2006

Abstract

The mechanical behaviour of a quasi-brittle cement concrete refractory, submitted to tensile cyclic and static loading was studied at room temperature. Delayed rupture was observed in the two configurations, but the analysis of the cycling amplitude and maximum stresses showed that the last is predominant. The material therefore appears as sensitive to what is sometimes called static fatigue. Acoustic emission was measured in situ and was shown to be directly related to non-linear deformation and therefore to damage. The cumulated acoustic emission event number evolution with time during static or cyclic loading shows a sigmoidal behaviour. The first part of the curve, with decreasing slope is associated to diffuse damage in the specimen. Then a concentration of the acoustic emission signals around the fracture plane is observed. This concentration operates at the inflexion point of the graph of the cumulated A.E. signal versus time, and corresponds to a macrocrack that develops to rupture. Acoustic emission could therefore be a mean of predicting the remaining life of the specimen.
© 2005 Elsevier Ltd. All rights reserved.

Keywords: Fatigue; Lifetime; Refractories; Concrete

1. Introduction

Refractory materials are divided into two categories: manufactured and monolithic materials. The former are supplied shaped and fired, and their properties are controlled and known before the installation but they present the drawback of higher installation cost. The latter which are supplied as raw materials that must be shaped and fired in situ represent lower installation cost and this is the reason why the proportion of monolithic material has increased these last years. This is the case of cement concrete materials, that can be easily manufactured in large parts of complicate shape. The drawback of such materials is that they are cured in situ and their properties depends drastically on the application.

The structure or microstructure of refractory concretes is complex but at a first view can be considered as millimetric grains in a matrix constituted of fines and cement. Their mechanical behaviour is strongly dependent on temperature. At high temperature, they exhibit visco-plasticity, which might be advantageous regarding brittleness. The evolution of room temperature properties is also complex since it depends on heat treatment temperature. A resistance fall off is generally observed in the temperature range of about 200–700 °C followed by an increase at high temperature due to consolidation.[1,2] The former is caused by thermal expansion mismatch between the so called matrix and the grains.[3] This also contributes to the quasi-brittle behaviour mostly observed on such materials at room temperature.[4–6] This behaviour in addition to the complex microstructure leads to damaging during loading, which has been shown in other materials to be sensitive to cyclic fatigue.[7–10] However, very little work has been conducted on the lifetime prediction of refractory materials submitted to cyclic loads.

Material duration can be predicted either by modelisation of cyclic fatigue or evaluation of the remaining potential life of the material through the measurement of a damage accumulation parameter. Owing to their microstructure the former might be difficult with refractories, but the measurement of damage is possible. Indeed, the detailed analysis of the mechanical behaviour shows first an increase of diffuse damage followed by a concentration of the damage around the fracture place, which leads to the initiation and propagation of a macro-crack. The first step of damage accumulation can therefore be a relevant indicator for lifetime prediction. This can be achieved by acoustic emission that can be easily linked to damage in such materials.[11–17]

The purpose of this work was to investigate the lifetime behaviour of a cement concrete refractory. Such a material was

* Corresponding author.
E-mail address: christian.olagnon@insa-lyon.fr (C. Olagnon).

0955-2219/$ – see front matter © 2005 Elsevier Ltd. All rights reserved.
doi:10.1016/j.jeurceramsoc.2005.11.003

submitted to tensile cyclic and static loading up to rupture, while the acoustic emission was measured. The measurements were achieved at room temperature but at the application temperature (900 °C), the behaviour of the materials is still quasi-brittle.

2. Experiments

2.1. Materials

The material is a Commercial Medium Cement Castable (MCC) dense concrete containing mainly alumina and silica (c.f. chemical composition in Table 1), supplied in dried mixtures ready to use. The maximum aggregate size is about 7 mm. The dry powders were first homogenised for 60 s in a mixer, before adding 7 wt.% of tap water and mixing it again for 3 min, giving a high viscosity paste. The concrete was subsequently poured in moulds to final shape on a vibratory table in order to avoid the excessive formation of bubbles or defects. The mixture was maintained in the moulds for 24 h at a humidity of 100HR% at room temperature to promote the cement cure. The specimen were then removed from the mould and dried at 110 °C for 48 h in an oven, before being heat treated at a rate of 50 °C/h, up to 900 °C with two dwell times of 3 h at 150 and 350 °C as recommended by the supplier.

2.2. Mechanical tests

For practical reasons, mechanical tests of refractory materials are mainly conducted in flexure and compression. However, the former present many difficulties or disadvantages when applied on non-linear materials. This is the case of concrete materials where intensive damage accumulation leads to non-linear stress–strain curves with asymmetric behaviour between traction and compression.[18] It is not possible to deduce the stress strain relation from flexure and it is probable that the compression part of the sample modifies the cyclic fatigue behaviour. The mechanical tests were therefore conducted in tension. For this purpose cylindrical specimens ($\phi = 32$ mm and $h = 100$ mm) were selected and the bases were carefully ground in order to achieve a very good parallelism. Two metallic parts were subsequently glued with epoxy resin to the specimens bases (Fig. 1). The whole device was fixed to the tensile machines through several perpendicular pin-hole systems. In order to check the alignment and in order to measure the real axial deformation, three strain gages were glued on the specimen surface. With those precautions, maximum deformation difference measured on a tensile specimen was lower than 8%, suggesting that the parasite bending was very small.

Table 1
Chemical composition of the material (supplier data)

	wt.%
Al_2O_3	51
SiO_2	42
Fe_2O_3	0.8
CaO	4.1

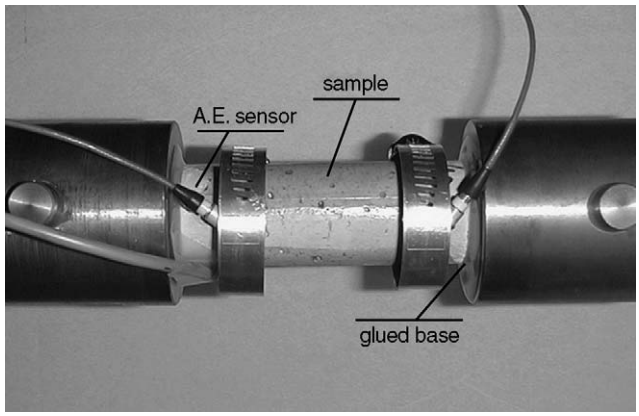

Fig. 1. Photograph of the tensile set up. The specimens is glued at the bases and the acoustic emission sensors are fixed by clamp collars.

2.3. Acoustic emission

The acoustic emission device is a commercial Mistras 2001 provided by Euro Physical Acoustics connected to two 40 dB pre-amplifiers and two resonant piezoelectric sensors (μ80). The maximum sensitivity of these sensors are between 100 kHz and 1 MHz, with a resonance peak at 250 kHz. The sensors were maintained on the two specimen ends by means of clamp collars and a grease couplant was disposed between the sensor and the specimen (Fig. 1). After fixing the sensors on the specimen, a pencil lead break procedure was applied to generate repeatable A.E. signals for the calibration.[19] It stimulates reproducible A.E. signals that make possible to calibrate the E.A. system and to measure the wave velocity (3600 m/s). Table 2 shows the typical settings of the A.E. system. The use of two sensors makes it possible to localise the events along the specimen axis, and brings the additional benefit that one can easily reject parasite or any events caused by the machine. The maximum time difference observed on the two sensors for a given acoustic emission source is equal to the ratio of the distance between the sensors to the wave velocity. Two signals observed on the two sensors with a time difference lower than the maximum time difference, are considered as localised, while the others are rejected. This localisation is therefore only a single axis, but still makes it possible to show that the damage is diffuse all along the specimen during the test.

Table 2
Typical settings of the AE acquisition system

Sampling rate (MHz)	8
Preamplifier gain (dB)	40
Threshold of detection (dB)	33
Type of sensor	Micro-80 PAC
Couplant	Wave guide and Silicon grease
PDT (peak definition time) (μs)	300
HDT (hit definition time) (μs)	600
HLT (hit Lockout time) (μs)	1000
Bandwidth (kHz)	100–1000
Wave velocity (m/s)	3600

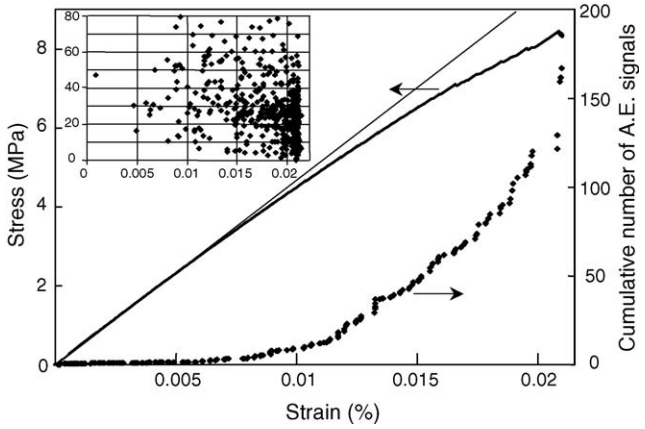

Fig. 2. Monotonic tensile stress–strain plot obtained at imposed velocity where the straight line is an extrapolation of the elastic slope, and cumulative number of acoustic emission signals. The imbedded small figure displays the localisation acoustic emission events along the tensile specimen as function of strain.

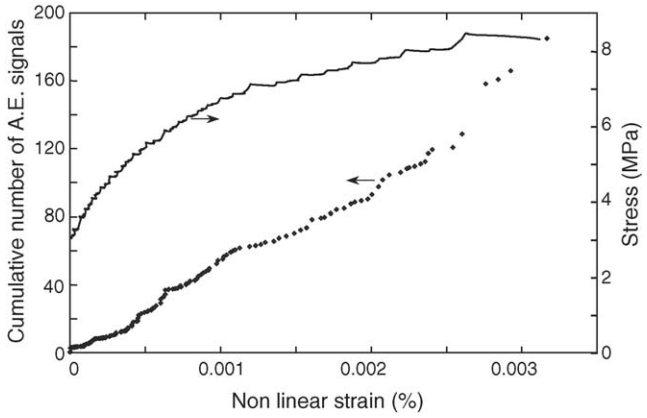

Fig. 3. Plot of the cumulative number of acoustic events and stress during a tensile test as function of the non-linear strain.

3. Results and discussion

3.1. Monotonic tensile behaviour

The static tensile monotonic stress strain behaviour of the material was measured to rupture at constant imposed displacement velocity and a typical example is displayed in Fig. 2. The mean fracture stress over 10 samples is equal to 8.2 MPa with a surprising standard deviation of 0.2 MPa. The behaviour is relatively linear up to the third of the fracture stress. This suggests an elastic behaviour in this range, which is confirmed by the absence of acoustic emission. Above this point, the behaviour is non-linear and the stiffness decreases, while acoustic emission occurs and increases with the non-linear behaviour. The analysis of the localisation of the acoustic signals along the sample axis shows that the sources are distributed all along the specimen for up to 70–80% of the fracture stress as shown in Fig. 2. This implies the existence of diffuse damage in this stress range. However, at the high end of loading a more important emission with larger peak intensities is observed at what will be the final fracture location. In order to show the evolution of acoustic emission with deformation, we have calculated the non-linear deformation by subtracting the linear deformation evaluated from the initial stress strain slope to the total deformation (Fig. 3). The evolution of the acoustic emission events with this non-linear deformation is nearly proportional up to fracture. This evolution was observed on each specimen tested. The number of acoustic events, although recorded in the same condition, with the same parameters was very dispersed from specimens to specimens. This shows that acoustic emission is a good method for recording damaging in the material. However, owing to the complex microstructure of the material, the direct observation of the damage is difficult, even by SEM. We can however suppose that it is mainly caused by microcracking. The fracture surfaces show that the larger aggregates are cleaved (Fig. 4).

3.2. Cyclic fatigue

Cyclic test have been conducted at a frequency of 0.1 or 1 Hz. The samples were loaded to a prescribed mean stress σ_m at constant loading rate, then cycling occurred with an amplitude A, up to rupture. The maximum selected stresses were relatively high compared to the material strength, since the purpose was to study fatigue during a moderate number of cycles. The acoustic emission was also continuously recorded during the experiments. Fig. 5 represents a typical example of cycling at a mean stress of 4 MPa and an amplitude of 1.5 MPa, i.e. a maximum stress equal to 67% of the mean fracture strength. On that graph the load is represented by discrete points solely when an AE event was recorded in order to show the stress level for which acoustic emission occurred. Clearly AE mostly appears at the highest part of the loading, but some signals are also observed in the low

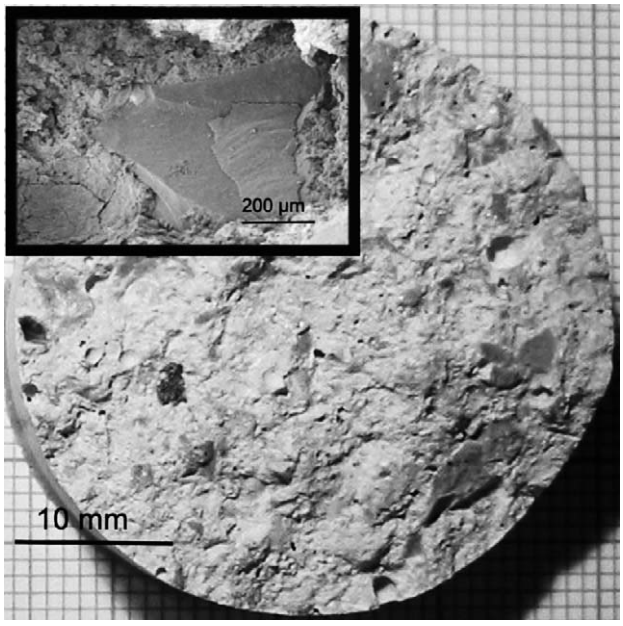

Fig. 4. Optical and SEM micrographs of a fracture surface, showing the cleavage of the aggregates.

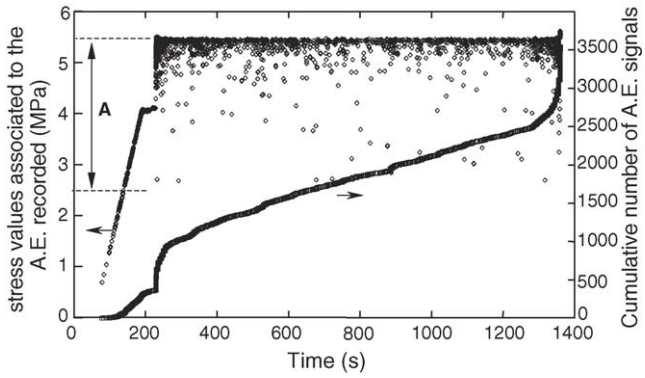

Fig. 5. Example of cyclic test conducted at an amplitude *A*. The stress, represented by points concomitant with acoustic events and the cumulative number of acoustic emission signals are plotted vs. duration.

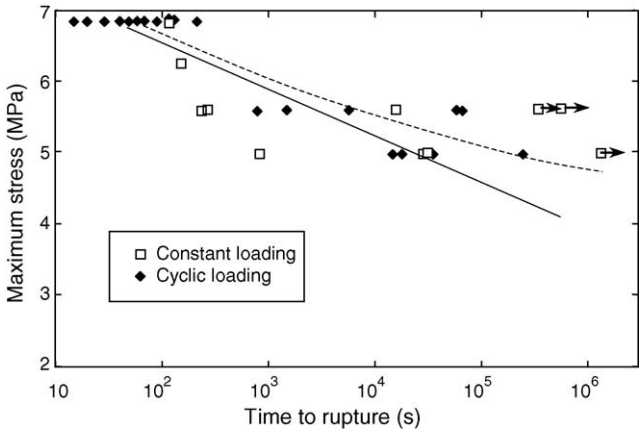

Fig. 7. Comparison of the static load and cyclic load, in terms of maximum stress vs. lifetime. Solid and dash lines are extrapolations of the cyclic and static results, respectively.

stress range. The evolution of the cumulated acoustic events is reproducible between different specimens and therefore interesting to analyse. As observed in the monotonic test, AE starts above a minimum stress, then, increases during loading up to the maximum stress, i.e. at the first cycle. The evolution of the cumulated acoustic events shows a sigmodal curve with a decrease of the derivative with respect to time, followed by an increase of this derivation that becomes strong just before breaking. Therefore, the damaging rate decreases during the first part down to a minimum value. Several mean stress and amplitude values have been tested and the results are represented in Fig. 6 either in terms of maximum stress or amplitude as function of time to rupture. Although the scattering is high, there are clearly some fatigue effects, inducing delayed fracture. Owing to the number of samples tested we were not able to make series of tests at constant amplitude or maximum stress. However, the relation seems more monotonic when plotting the maximum stress. This is in contradiction to what is observed with metals where the cycling amplitude is of major importance, but this is rather similar to what has been measured on technical ceramics. The group of specimens tested at the highest maximum load all show a very short time to failure. For these, the lifetime is rather

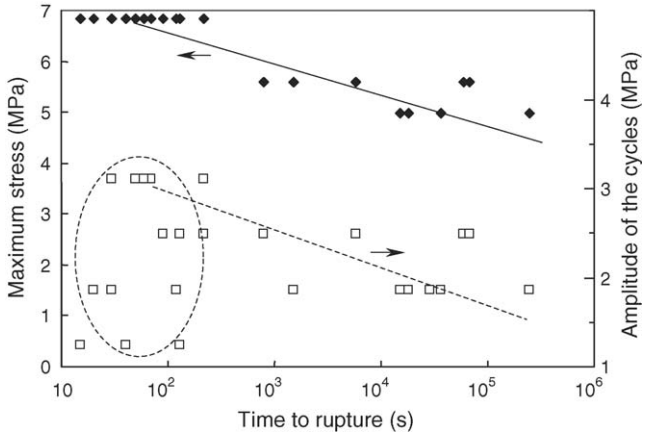

Fig. 6. Plot of the maximum stress or amplitude vs. fracture time for cyclic fatigue tests. The lines are not a best fit, but a gross indication of the evolution.

insensitive to amplitude. Indeed those corresponding data do not show any significant tendency. This reinforces the idea that the maximum load is the main parameter driving fatigue. It can be stated that when the maximum stress is high, the importance of the amplitude is low. This is the reason we have conducted tests at constant stress, so called "static fatigue" tests, where only the maximum stress can play a role (Fig. 7). Such tests are current in ceramics and acknowledged as leading to significant lifetime dispersion. In the case of refractories the dispersion is even higher, probably because of the complex microstructure. The durations are typically in the range of 400 s to several weeks for a stress of 5.5 MPa, i.e. 66% of the fracture stress. However, there is clearly a "static fatigue" effect with increased lifetime with a decrease of the applied stress. Note that the arrows in Fig. 7 represent specimens that have failed due to an incident of either the tensile machine or the electric power. Their points therefore represent only the lower limit of the real duration. On the same graph we have superposed the cyclic fatigue results to show that in a first approximation these results are very similar to those of the maximum stress cyclic fatigue, showing the importance of this parameter in the cyclic fatigue. However, considering a more detailed analysis and that three of the static results have been interrupted before the end, suggests that the average cyclic plot is slightly shifted to the left of the static one. If there were no cyclic effect, the delayed rupture due to cyclic loading under a pure maximum stress effect, would lead to longer duration (material submitted for a shorter duration to a high stress). In such a case, the cyclic graph should be shifted to the right of the static one, which is probably not the case here. We can therefore suggest that if the maximum stress is indeed the most significant parameter, there is still a moderate cyclic effect.

Fig. 8 represents a typical cumulated acoustic emission during a "static loading test". The evolution is quite similar to that observed on a cyclic loading graph. Again a sigmoidal graph is observed, with a strong increase of the acoustic events after a minimum rate. The plot of the acoustic emission with time is similar for the monotonic, cyclic and static tests. An example for

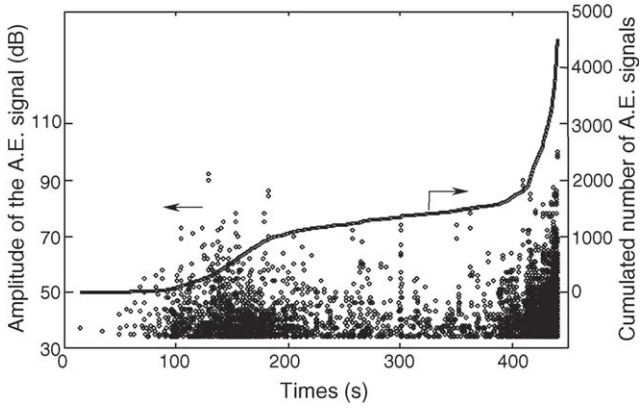

Fig. 8. Example of static test. Cumulative acoustic emission signals and amplitudes of events as function of time.

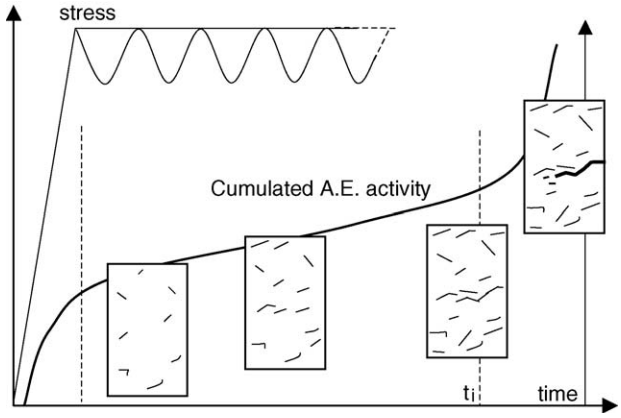

Fig. 10. Schematic drawing showing the cumulative acoustic emission signals and the load, function of time.

the static test displayed in Fig. 8 is given in Fig. 9. As mentioned above, the damaging is diffused up to the inflection point, then the damage distribution is centred around the rupture point.

3.3. Discussion and mechanisms

These results and analyses clearly show that such materials are submitted to fatigue, and sensitive to both amplitude and maximum stress. The same behaviour has been observed in polycrystalline ceramics exhibiting toughening interaction on cracking such as coarse grain alumina or zirconia. The fatigue mechanism is due to the conjunction of both stress corrosion cracking and toughening. The crack propagation by stress corrosion is directly linked to maximum stress intensity factor and hence maximum stress that causes delayed fracture. Toughening (generally crack bridging, phase transformation, microcracking) reinforces the material, but is mainly associated with friction and other dissipative mechanisms. Thus during alternate loading and unloading these mechanisms are submitted to degradation, which in turn reduces the toughening extent. Therefore, cycling leads to decrease of lifetime as compared to the same material submitted to a constant stress equal to the maximum cycling stress. In the end the crack velocity is directly linked to an equilibrium between stress corrosion cracking and toughening degradation. Crack velocity and therefore lifetime can be related primarily to maximum stress and to a lower extent to amplitude.

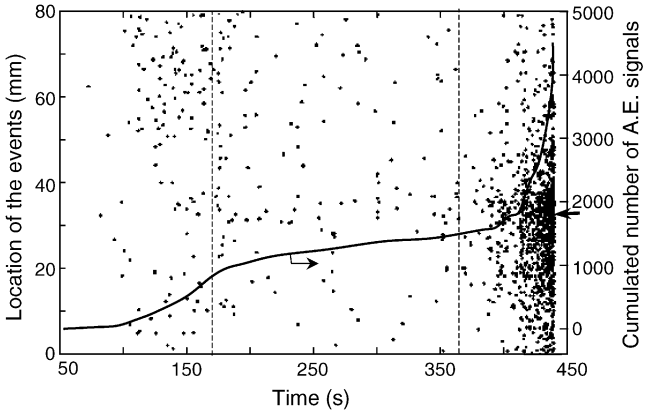

Fig. 9. location of the acoustic emission event along the specimen axis as a function of time during the static load of Fig. 6. The arrows shows the rupture location. The associated cumulative acoustic emission signals is superimposed.

In terms of lifetime, the behaviour of the concrete refractory is similar, but more complex because they do not exhibit brittle behaviour. In polycrystalline ceramics the development of a defect to become a propagating mature crack is relatively short and lifetime for these ranges is mostly controlled by propagation. In refractories, at least with the specimen size studied here, most of the lifetime is controlled by the development of a macrocrack and therefore damage accumulation. However, a qualitative description can be made since we have shown that acoustic emission can be related to damage accumulation. Three parts can be considered in the typical curve displayed in Figs. 5 and 8, as schematically drawn in Fig. 10. We can consider that there already exist some defects such as cavities, or microcracks in the material of size distribution $f_a(a)$. Because of the heterogeneities in the material, these defects are submitted to a stress field distribution during loading. On a simple approach, it can be characterised by a stress concentration k defined as local stress brought about by the applied stress, thus a distribution $f_k(k)$. The product of these two probability densities gives what corresponds to some crack criticality distribution that can be theoretically related to stress intensity factor. During the initial loading (first part of the graph), the most critical defects will initiate or propagate first. The higher the load the larger the number of defects concerned, which explains the rising acoustic emission activity. At this point the acoustic emission signals are due to both initiation of cracks and propagation of previously initiated cracks that give a delayed effect on damage. The number of microcracks present in the material increases with the load. In the second part, the load is either constant or lower than the maximum value in the case of cyclic fatigue. The crack initiation rate decreases. The propagation or the initiation of microcracks is due to delayed propagation of crack that are less and less critical. However, the cumulated acoustic emission events and therefore the number of microcracks still increases. At this point the acoustic emission is probably mainly caused by the propagation rather than by the initiation. The inflexion point

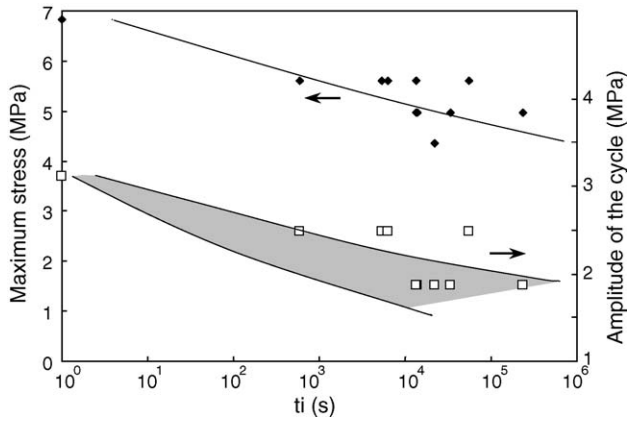

Fig. 11. Phenomenological modelisation (solid line and shaded area) of the cyclic fatigue in terms of the time t_i, and comparison to experimental results.

corresponds to an increase of acoustic emission activity in a particular zone and therefore to the concentration of the damage. Either the microcrack (or microcavity) density reaches a critical value or the equivalent length is larger than a critical value. The emission is caused both by the propagation of the macrocrack and by the initiation of microcracks in its process zone. In the present case of a small specimen, rupture occurs when this macrocrack reaches the sample edge or when it becomes unstable.

Fatigue of polycrystalline ceramics has been advantageously described in terms of a modified Paris law according to[8–9]:

$$\frac{da}{dN} = A K_{\mathrm{Imax}}^{m} \Delta K_{\mathrm{I}}^{n} \quad (1)$$

where K_{Imax} and ΔK_{I} are respectively the maximum stress intensity factor and the amplitude, N the number of cycles and A, m and n constants depending on the material and the mechanism. Integration of such a law from initial to critical crack length gives a relation between lifetime and the above parameters or their macroscopic equivalent, i.e. maximum and amplitude stresses as:

$$t_{\mathrm{f}} = B \sigma_{\mathrm{max}}^{a} \Delta \sigma^{b} \quad (2)$$

where the exponents a and b are related to m and n. In the case of refractories the basic mechanisms are probably similar, but more complex due to the existence of microcracking, the lifetime being therefore mostly controlled by the initiation of the macrocrack.

A similar phenomenological description can however be made, by replacing the time to failure by the time to initiate a macrocrack, i.e. at the inflexion point t_i in Eq. (2). Such an analysis is represented in Fig. 11 where the parameters a and b have been fitted by the least mean square method. The predicted times have been calculated for the different experimental amplitude and maximum stresses. The description is far from being perfect, especially when plotting the amplitude where the dispersion is given by the shaded area. However, it still can give a rough estimation of the time t_i, as a function of the two stress parameters.

On real components loaded with an imposed strain where long cracks can be stable, the propagation to a critical size can also control the lifetime. However, in other cases the determination of the inflection point can be relevant to estimate the remaining life of the component. For this purpose, acoustic emission can be monitored in situ in critical applications.

4. Conclusion

The lifetime of a quasi-brittle cement concrete refractory, submitted to tensile cyclic and static loading was studied at room temperature. Both the maximum value and the amplitude of the cyclic stress played a role, but the former was more prominent. This was confirmed by the delayed rupture observed under static loading. The acoustic emission, measured in situ was shown to be directly related to non-linear deformation and therefore to damage. The cumulated acoustic emission event number evolution with time during static or cyclic loading shows a sigmoidal behaviour. The first part of the curve, with decreasing slope is associated to diffuse damage in the specimen. Then the damaged becomes localised, leading to an increasing slope, with the formation of a macrocrack that develops to rupture. Acoustic emission can therefore be a mean of predicting the remaining life of the specimen.

Acknowledgment

The authors wish to acknowledge Electricité de France (EDF) for their financial support and their interest in the work.

References

1. Parker, K. M. and Sharp, J. H., Refractory calcium aluminate cement. *Trans. J. Br. Ceramic Soc.*, 1982, **81**(5), 35–42.
2. Bazant, Z. P. and Kaplan, M. F., *Concrete at High Temperatures. Material Properties and Mathematical Models, Concrete Design and Construction Series*. Longman Group, London, 1996.
3. Simonin, F. PhD thesis, Comportement thermomécanique de bétons réfractaires alumineux contenant du spinelle de magnésium, Institut National des Sciences Appliquées de Lyon, N°2000 ISAL 0043, 2000, 165 p. (in French).
4. Jensen, D. and Chatterji, S., State of the art report on microcracking and lifetime of concrete – Part I, Rilem technical committees, TC-122-MLC. *Matériaux et Constructions/Materials and Structures*, 1996, **29**, 3–8.
5. Harmuth, H., Rieder, K. and Krobath, M., Investigation of the non-linear behaviour of ordinary ceramic refractory materials. *Mater. Sci. Eng.*, 1996, **A214**, 53–61.
6. Henderson, R. J. and Chandler, H. W., The non-linear mechanical behaviour of high performance refractories. *Key Eng. Mater.*, 1997, **132–136**, 504–507.
7. Dauskardt, R., Yu, W. K. and Ritchie, R. O., Fatigue crack propagation in transformation toughenend zirconia ceramics. *J. Am. Ceram. Soc.*, 1987, **70**(10), 246–252.
8. Liu, S. and Chen, I.-W., Fatigue of yttria-stabilized zirconia. I. Fatigue damage, fracture origins and lifetime prediction. *J. Am. Ceram. Soc.*, 1991, **74**(6), 1197–1205.
9. Liu, S. and Chen, I.-W., Fatigue of yttria-stabilized zirconia. II. Crack propagation, Fatigue striation and short-crack behaviour. *J. Am. Ceram. Soc.*, 1991, **74**(6), 1206–1216.
10. Chevalier, J., Olagnon, C. and Fantozzi, G., *J. Am. Ceram. Soc.*, 1999, **82**(11), 3129–3138.

11. Maliszkiewicz, P., Behaviour of concrete observed by acoustic emission measurement. *Mater. Sci. Forum*, 1996, **210–213**, 479–486.
12. Spooner, D. C. and Dougill, J. W., A quantitative assessment of damage sustained in concrete during compressive loading. *Magazine Concrete Res.*, 1975, **27**(92), 151–160.
13. McCabe, W. M., Körner, R. M. and Lord, A. E., Acoustic emission behavior of concrete laboratory specimens. *ACI J.*, 1976, **73**, 367–371.
14. Tanigawa, Y., Yamada, K. and Kiriyama, S. I., Relationship between fracture mode and acoustic emission characteristics of mortar. In *The 24th Japan congress on Materials Research–Non Metallic Materials*, 1981, pp. 241–247.
15. Tang, C. A., Liu, H., Lee, P. K. K., Tsui, Y. and Tham, L. G., Numerical studies of the influence of microstructure on rock failure in uniaxial compression. *Int. J. Rock Mechan. Mining Sci.*, 2000, **37**, 555–569.
16. Uomoto, T., Application of acoustic emission to the field of concrete engineering. *J. Acoustic Emission*, 1987, **6**(3), 137–143.
17. Li, F. and Li, Z., Acoustic emission monitoring of fracture of fiber reinforced concrete in tension. *ACI Mater. J.*, 2000, **97**(6), 629–636.
18. Simonin, F., Olagnon, C., Maximilien, S. and Fantozzi, G., Room temperature quasi-brittle behaviour of an aluminous refractory concrete after firing. *J. Eur. Ceram. Soc.*, 2002, **22**, 165–172.
19. Nielsen, A., *Acoustic Emission Source Based on Pencil Lead Breaking*, *vol. 80*. The Danish Welding Institute Publication, 1980, p. 15.